Czech Technical University in Prague

Faculty of Electrical Engineering

Department of Circuit Theory

Model of Piezoelectric Power Supply for Use in Biomedicine

Bachelor's thesis

Study program: Bachelor

Field of study: Medical Electronics and Bioinformatics

Work supervisor: Prof. Ing. Miroslav Husák, CSc.

Martin Lisý

Prague 2023

ZADÁNÍ BAKALÁŘSKÉ PRÁCE

I. OSOBNÍ A STUDIJNÍ ÚDAJE

Příjmení: **Lisý** Jméno: **Martin** Osobní číslo: **494714**

Fakulta/ústav: **Fakulta elektrotechnická**

Zadávající katedra/ústav: **Katedra teorie obvodů**

Studijní program: **Lékařská elektronika a bioinformatika**

II. ÚDAJE K BAKALÁŘSKÉ PRÁCI

Název bakalářské práce:

Model piezoelektrického napájecího zdroje pro využití v biomedicíně

Název bakalářské práce anglicky:

Model of Piezoelectric Power Supply for Use in Biomedicine

Pokyny pro vypracování:

1. Shrňte poznatky z literatury o využití piezoelektrických elementů pro napájení biomedicínských aplikací.
2. Navrhněte model napájecího zdroje s piezoelektrickým elementem, popř. s více elementy, pro realizaci zvolte vhodný typ (y) piezoelektrického elementu, integrovaný obvod pro management a ukládání získané energie. Navržený zdroj realizujte ve formě laboratorního vzorku. Jako zdroj mechanického pohybu uvažujte např. otřesy při pohybu lidského těla, pohyby končetin nebo např. došlap boty.
3. Změřte dosažené parametry realizovaného modelu zdroje, tj. zejména výstupní napětí, výstupní proud, výstupní výkon v závislosti na zatěžovacím odporu a frekvenci mechanického buzení, stanovte optimální zatěžovací odpor pro největší výstupní výkon a proud, stanovte optimální dosaženou mechanickou budicí frekvenci apod.
4. Navrhněte možné úpravy pro vylepšení účinnosti systému.

Seznam doporučené literatury:

1. Neumann, P., Uhlíř, J.: Elektronické obvody a funkční bloky I, II, ČVUT.
2. Husák, M., Autonomní mikronapájecí zdroje s piezoelektrickým principem, DPS, 9-10/2013, str. 2, ISSN 1805-5044
3. Husák, M., Autonomní mikronapájecí zdroje s piezoelektrickým principem - II, DPS, 11-12/2013, str. 2, ISSN 1805-5044
4. Husák, M., Piezoelektrické mikro- a nanogenerátory, DPS, 1-2/2014, str. 2, ISSN 1805-5044

Jméno a pracoviště vedoucí(ho) bakalářské práce:

prof. Ing. Miroslav Husák, CSc. katedra mikroelektroniky FEL

Jméno a pracoviště druhé(ho) vedoucí(ho) nebo konzultanta(ky) bakalářské práce:

Datum zadání bakalářské práce: **31.01.2023** Termín odevzdání bakalářské práce: **26.05.2023**

Platnost zadání bakalářské práce: **22.09.2024**

prof. Ing. Miroslav Husák, CSc.	doc. Ing. Radoslav Bortel, Ph.D.	prof. Mgr. Petr Páta, Ph.D.
podpis vedoucí(ho) práce	podpis vedoucí(ho) ústavu/katedry	podpis děkana(ky)

III. PŘEVZETÍ ZADÁNÍ

Student bere na vědomí, že je povinen vypracovat bakalářskou práci samostatně, bez cizí pomoci, s výjimkou poskytnutých konzultací. Seznam použité literatury, jiných pramenů a jmen konzultantů je třeba uvést v bakalářské práci.

Datum převzetí zadání Podpis studenta

Declaration

„I declare that the presented work was developed independently and that I have listed all sources of information used within this work in accordance with the methodical instructions for observing the ethical principles in the preparation of university theses.“

Prague, 12.05.2023.

Martin Lisý

Acknowledgments

I wish to thank my supervisor prof. Ing. Miroslav Husák, CSc. for his advice and assistance throughout creating this thesis and for his flexibility when presented with an unexpected outcome.

I also wish to thank my family and friends for aiding me through hard times to the end of the bachelor's programme.

Lastly, I would like to thank Ing. Jiří Kroutil, Ph.D. and Ing. Alexandr Laposa, Ph.D. for assisting me with my measurements.

Abstract

Piezoelectric devices have nowadays rising applications in many fields including biomedicine. An important part of creating these biomedical devices is the knowledge of piezoelectrical properties and principles. Staying up to date with these novelty applications enables creating new devices or upgrading current devices. This thesis presents piezoelectric properties and principles as well as recent developments of piezoelectric use in biomedicine. It uses this knowledge in designing a piezoelectric harvester model with focus on the parameters of its piezoelectric generator. This thesis also states measuring steps and issues encountered that hindered completing the model.

Key words

Piezoelectric harvester, biomedical applications, model design.

Abstrakt

Piezoelektrická zařízení mají v dnešní době rostoucí využití v mnoha oborech včetně biomedicíny. Důležitou součástí pro návrh a realizaci takových zařízení je znalost piezoelektrických vlastností a principů. Zůstáním v obraze o těchto novotách umožňuje vytvořit nová zařízení, případně vylepšit současná zařízení. Tato práce představuje piezoelektrické vlastnosti a principy a současné inovativní využití piezoelektrik v biomedicíně. Tyto znalosti využívá k návrhu modelu piezoelektrického sběru energie, se zaměřením na vlastnosti piezoelektrického zdroje. Tato práce dále představuje postup měření a popisuje problémy, které zabránily v dokončení modelu.

Klíčová slova

Piezoelektrický sběr energie, zařízení v biomedicíně, návrh modelu.

Table of Contents

List of Figures

List of Tables

List of units

Physical quantity	Name	Unit
$\vec{P}$	Polarisation	C/m^2
$\vec{p}$	Dipole moment	C.m
q	Elemental charge	C
$\vec{x}$	Distance	m
V	Volume	m^3
Q_b	Bound charge	C
$S, \Delta S, d\vec{S}$	Surface area	m^2
$\vec{D}, D$	Electric displacement vector, matrix	C/m^2
ε	permittivity	F/m
$\vec{E}, E$	Electric intensity vector, matrix	N/C
S	Strain	-
s^E	Elastic compliance constant	m^2/N
T	Stress	N/m^2
d	Coefficient for strain with respect to electric charge	C/N
e	Coefficient for stress with respect to electric charge	C/N
g	Coefficient for strain with respect to voltage	V.M/N
h	Coefficient for stress with respect to voltage	V.M/N
k	Electromechanical coupling factor	-
C	Capacitance	F
V	Voltage	V
F	Force	N
I	Current	A
Z	Impedance	Ω

List of abbreviations

Abbreviation	Name
PZT	Lead Zircon Titanate
PVDF	Polyvinylidene-fluoride
PVDF-TrFE	Polyvinylidene-fluoride-trifluoro ethylene
EH	Energy Harvester
PeMG	Piezoelectric Micro Generator
PeNG	Piezoelectric Nano Generator
PeM/NG	Piezoelectric Micro or Nano Generator
UFEH	Ultra Flexible Energy Harvester
ACF	Anisotropic Conductive Film
PEH	Piezoelectric Energy Harvester
UVLO	Undervoltage Lockout
PGOOD	Power GOOD
RMS^2	Root-Mean-Squared to the second power, Power of a signal
VMCU	Voltage Microcontroller Unit
p-p	Peak-to-Peak

Chapter 1: Introduction

This chapter describes the piezoelectric effect, focusing on its mathematical, physical, and material properties.

1.1 The Piezoelectric effect

The piezoelectric effect is widely used in micro and nano devices as a power source. The direct piezoelectric effect was first discovered by brothers Pierre and Jacques Curie in 1880 [1]. Their experiments on different crystal materials showed that when under mechanical stress, these crystals electrically polarise, and the polarisation is proportional to the applied stress [2]. The converse piezoelectric effect, materials showing a geometric strain under an applied electric field, was discovered by Gabriel Lippman a year later, in 1881 [3].Not all crystal materials show piezoelectric properties as the effect is limited to a small class of materials [1].

1.2 The description of polarisation

A charge generated in piezoelectric materials is dependent on the polarisation of such materials. Under stress, piezoelectric materials will create electric dipoles, pairs of equal positive and negative charges. These dipoles are described by a vector $\vec{p}$ called the dipole moment given as $\vec{p} = q \cdot \vec{x}$ (1). Where q is the charge and $\vec{x}$ is the distance between the positive charge and the negative charge. If we sum or integrate all the electric dipoles in a piezoelectric material, we get the total polarisation $\vec{P}$. Mathematically, this can be expressed as:

$$\vec{P} = \lim_{\Delta V \to 0} \frac{\sum_{\Delta V} \vec{p}}{\Delta V} \tag{2}$$

ΔV symbolises an element of volume.

If we assume that a polarised material has N dipoles in an element of volume, we can rewrite eq. (2) as:

$$\vec{P} = \frac{N \cdot \vec{p}}{\Delta V} = \frac{N \cdot q \cdot x}{\Delta S \cdot x} = \frac{N \cdot q}{\Delta S} = \frac{\Delta Q_b}{\Delta S} \tag{3}$$

Where ΔQ_b symbolises the bound charge in an element of volume and ΔS is the surface area of this element.

Equation (3) now gives us a total bound charge created by polarisation:

$$\Delta Q_b = \vec{P} \cdot \Delta S \rightarrow \mathrm{d}Q_b = \vec{P} \cdot d\vec{S} \rightarrow Q_b = \iint_S \vec{P} \cdot d\vec{S} \tag{4}$$

Polarisation is also defined with electric displacement $\vec{D}$ and electric intensity $\vec{E}$ as:

$$\vec{P} = \vec{D} - \varepsilon \vec{E} \tag{5}$$

Where ε is permittivity. [4], [5]

Equation (5) is used for describing polarisation in piezoelectric materials later in this text (12).

1.3 Piezoelectric equations

The piezoelectric effect is described by several tensor equations, the two most significant are the equation for "Strain" (6) and the equation for "Electric charge displacement" (7) shown in matrix form.

$$S = s^E \cdot T + d^t \cdot E \tag{6}$$

Where S is the strain matrix, s^E is the elastic compliance constant, T is stress, d^t is the transposed matrix of piezoelectric strain coefficients and E is the electric intensity.

$$D = d \cdot T + \varepsilon \cdot E \tag{7}$$

Where D is electric displacement, d is the matrix of piezoelectric coefficients, T is stress, ε is permittivity and E is the electric field [6], [7].

1.4 Coefficient deduction

The piezoelectric effect is also described by four significant coefficients [6]. Each coefficient relates mechanical properties to electrical properties or vice versa. They are:

The coefficient for strain with respect to electric charge d_{ij} given as:

$$d_{ij} = \left(\frac{\partial D_i}{\partial T_j}\right)^E = \left(\frac{\partial S_j}{\partial E_i}\right)^T \tag{8}$$

The coefficient for stress with respect to electric charge e_{ij} given as:

$$e_{ij} = \left(\frac{\partial D_i}{\partial S_j}\right)^E = -\left(\frac{\partial T_j}{\partial E_i}\right)^S \tag{9}$$

The coefficient for strain with respect to voltage g_{ij} given as:

$$g_{ij} = -\left(\frac{\partial E_i}{\partial T_j}\right)^D = \left(\frac{\partial S_j}{\partial D_i}\right)^T \tag{10}$$

The coefficient for stress with respect to voltage h_{ij} given as:

$$h_{ij} = -\left(\frac{\partial E_i}{\partial S_j}\right)^D = -\left(\frac{\partial T_j}{\partial D_i}\right)^S \tag{11}$$

Where all can be derived from equations (6) and (7) when modified into their desired forms. These modifications will not be presented in this text. Each coefficient is given in its element formulation.

Another important coefficient is the electromechanical coupling factor k. It describes the ratio of converted energy to input energy. It is given either as:

$$k^2 = \frac{mechanical\ energy\ converted\ to\ electric\ energy}{input\ mechanical\ energy} \tag{12}$$

Or as:

$$k^2 = \frac{electric\ energy\ converted\ to\ mechanical\ energy}{input\ electric\ energy} \tag{13}$$

Depending on the direct or converse piezoelectric effect, respectively [3].

Each axis of a piezoelectric element has its unique value, but factors k_{33} and k_{31}, just as d_{33}, d_{31} and g_{33}, g_{31} are the more important ones. Some typical values are presented later in this text.

1.5 Generated voltage

When extracting charge from a piezoelectric element, we need an efficient transformational circuit. A basic electrical equivalent circuit's (Figure 1) voltage is deducted in the upcoming chapter.

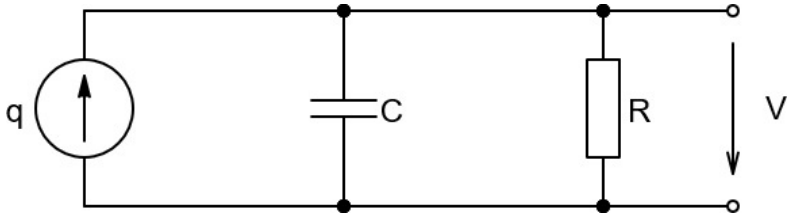

Figure 1. A basic electrical equivalent circuit of a piezoelectric element [2].

If we rewrite equation (5) with respect to electric displacement D, and compare the result with (7), we get:

$$P = d \cdot T \tag{14}$$

This equation is a mathematical expression of the direct piezoelectric effect. When substituting equation (14) into (4), we get the relationship between generated charge and the stress applied to a piezoelectric material:

$$Q_b = \iint_S d \cdot T \cdot d\vec{S} \tag{15}$$

Stress T and piezoelectric coefficients d are given in their matrix forms.

If we allow ourselves a simplification of an, ideally, homogenous material and a fixed surface area, we can transform equation (15) to:

$$Q_b = d \cdot T \cdot S \tag{16}$$

From equation (16) we can derive the output voltage shown in Figure 1 as a function of Force:

Using the facts that $Q = C \cdot V$, charge is equal to capacity times voltage, and that $T = \frac{F}{S}$, stress is equal to force divided by surface area, substituting into (16) we get, with relation to time, as both charge and voltage are time dependant:

$$Q(t) = d \cdot \frac{F}{S_i} \cdot S_j = C \cdot V(t) \tag{17}$$

Where indexes i and j represent possibly different orientations of surfaces.

Rewriting (17) with respect to voltage and assuming constant surface area:

$$V(t) = d \cdot \frac{F}{C \cdot S_i} \cdot S_j = const. \cdot F(\mathrm{t}) \tag{18}$$

Equation (18) highlights the simplicity of using piezo electrics as a power source: Generated voltage is, regarding the earlier simplifications, equivalent to force (pressure) applied to a piezoelectric element [2], [8]

1.6 Piezoelectric materials

Current progress in the field of piezoelectric devices is bound to the development of piezoelectrically better materials. As aforementioned, the Curie brothers first started their experiments with piezoelectricity and that on single crystal quartz (SiO_2). As we know, this led to the discovery of piezoelectricity. Broader experiments were carried out during World War I, where Dr. Paul Langevin created a quartz and Rochelle salt based acoustic transmitter as an attempt to locate German submarines. Although a revolutionary device, Rochelle salt is temperature dependant and water soluble. This eventually led to its replacement with lead zircon titanate ($PbZrTiO_3$, PZT) and barium titanate ($BaTiO_3$). Another important discovery was presented in 1969 by Kawai and Kureha. They showed the piezoelectric properties of polyvinylidene difluoride (PVDF) which is the basis of PVDF-TrFE, a commonly used piezoelectric [3].

Such materials and their composites are today the basis of piezoelectric devices. However, these materials are constantly improved, as we seek better piezoelectric properties and easier or cheaper material production. A recent trend has become creating piezoelectric biodegradable materials [9] that promise greater suitability for living tissue, as most used piezoelectric materials are nonorganic. Organic materials allow us to create flexible and textile-like materials showing piezoelectric properties. These materials, but mostly their properties and methods of creation are discussed in the upcoming chapter.

1.7 Currently used materials

The electrical properties of piezoelectrical materials are defined by their coefficients. Knowing the value of these coefficients is a key factor when creating a piezoelectric-based device. Table 1 shows the typical coefficient values of piezoelectric materials. The most used material for biomedicine is PZT as it has the highest d_{33} and k. PZT being a compound of lead may question its biocompatibility. However, it isn't an issue in biomedicinally used devices, as the amount of lead in a device is small. Issues may arise when trying to upgrade these devices to larger body surfaces. Polymer materials and their composites such as PVDF, are better suitable for our bodies, as they are not physiologically toxic.

A materials electro-mechanical properties correspond to its microscopic structure. Because of this, different methods are used to create enhanced materials. The most common are electro-spinning and spin casting. Figure 2 shows piezoelectric materials under an electron microscope.

Table 1. Common piezoelectric materials and their typical coefficient values [2], [10], [11].

Property	**$PbZrTiO_3$**	**$BaTiO_3$**	**PVDF**	**PZT-5A**
d_{33} (10^{-12} C/N)	370-590	149	-33	374
d_{31} (10^{-12} C/N)	110	78	23	-171
g_{33} (10^{-12} V.m/N)	19-25	14.1	330	24.8
g_{31} (10^{-12} V.m/N)	10	5	216	-11.4
k_{33} (-)	0.7 - 0.75	0.48	0.15	0.72
k_{31} (at 1 kHz)	0.30	0.21	0.12	0.61
Density (kg/m^3)	7500	5700	1780	7500
ε_r (-)	1200	1700	12	3400

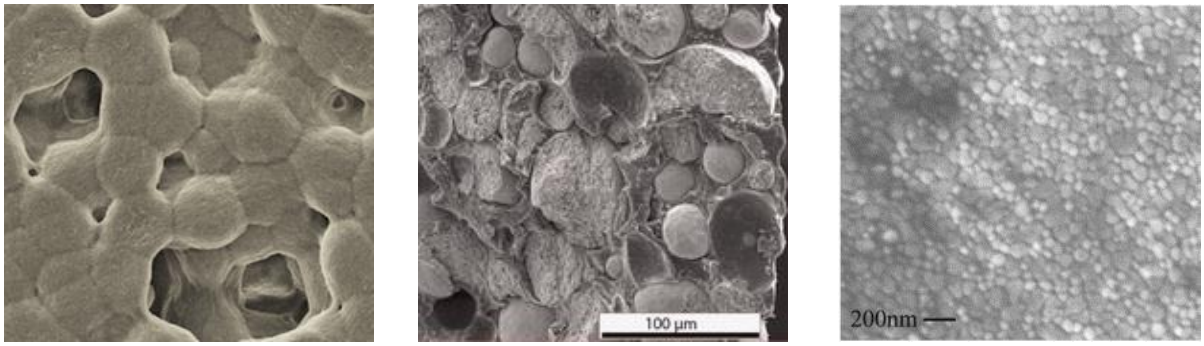

a **b** **c**

Figure 2. Piezoelectric materials under a scanning electron microscope.

a - 3 µm PVDF [12], b - PZT/epoxy composite film [13], c - PZT granite thin film [14].

Chapter 2: Piezoelectric Energy Harvesters and Devices in Biomedicine

This chapter describes piezoelectric harvesters and presents piezoelectrically powered devices in biomedicine. These devices consist of sensors, pacemakers, and energy harvesters.

2.1 Energy harvesters and generators

Due to its dimensional and electrical properties, the piezoelectric effect is widely used in constructing sensors, actuators or in the creation of intricate power sources called "Energy-Harvesters" (EH). These micro and nano-generators are widely used in biomedicine, but also in many other fields. The principle of an EH is to "harvest" an external energy (mechanical, chemical, thermal etc.) and transform it to an electrical output, such as current or voltage. A piezoelectric EH or a piezoelectric micro or nano-generator (PeMG or PeNG) takes mechanical energy, usually in the form of mechanical stress or strain, and transforms it to electric charge which can then be transformed with an integrated circuit to voltage or current or both. This is using the direct piezoelectric effect. If the PeMG or PeNG is based on the inverse piezoelectric effect, it creates some form of motion or deformation under an applied electric field. For instance, a piezoelectric motor can move a piece of material when under current. More information on piezoelectric motors can be found in [15].

2.2 Working principle of PeNGs/PeMGs

When constructing an EH, the main power source is a PeNG or PeMG. The principal factor in choosing what piezoelectric generator to use is its way of converting strain, stress to energy. In general, pressure applied to the generator deforms (bends, compresses, slides etc.) its elements (Figure 3), creating a charge that can then be harvested. The size of the output charge depends on the direction of the applied force. These properties are described by piezoelectric coefficients mentioned in chapter 1.4. A typical structure for PeM/NGs is a beam, as bending a material is simple to execute and bending a beam combines both compressive stress and shear stress, thus utilising d_{33} and d_{31} values, which are usually the highest. Another use for PeM/NGs is constructing sensors and actuators. They are often used as indicators or "helper elements" in many applications including biomedicine.

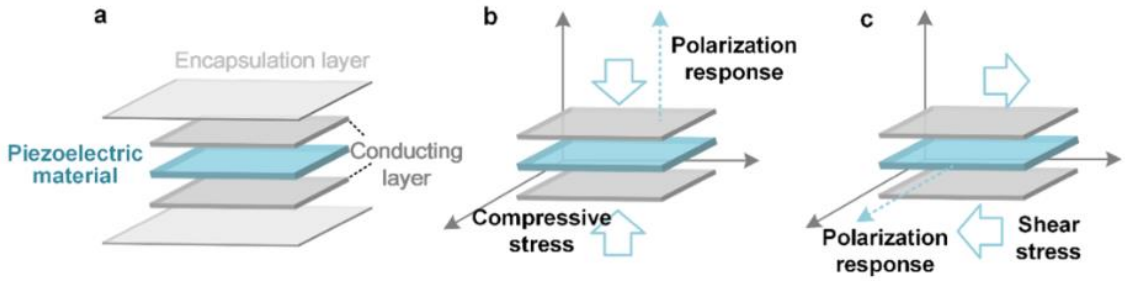

Figure 3. The general structure of a piezoelectric micro or nanogenerator [9].

a - the structure of a typical PeNG, b - polarisation response to compressive stress, c - polarisation response to shear stress.

2.3 Recent development in biomedicine

Piezo electronics are nowadays commonly used in biomedicine. The recent development in this field has brought many new, promising designs and technologies for the enhancement of our lives. They cover a large span of medical fields such as: cardiology, with new pacemakers [16], endoscopy: with new tumour sensing [17] and many more. These innovations are presented in this chapter.

2.3.1 Eye blinking detection

With the rapid increase of digital technologies in our daily lives such as phones, televisions and personal computers, our eyes are strained more than necessary. Eye fatigue in the form of inconsistent or infrequent blinking can indicate health problems like sleep deprivation, brain disease and many others. Kim et al from the university of Houston presented [18] a multi-layered flexible piezoelectric eye movement sensor applicable on the temple or on eyelids capable of distinguishing between fully open, closed, and semi-closed eyelids (Figure 4). This sensor is also capable of recognising lateral eye movement as in left, right, or neutral (centre) and the speed of this movement. The output voltages from these movements range from 120 mV when attached to the temple, to 20 mV when attached to the lower eyelid [18].

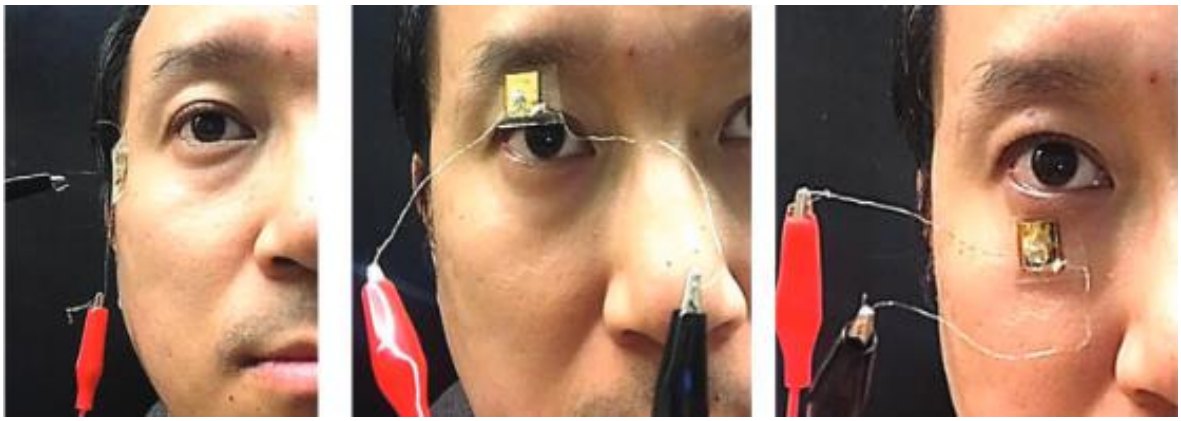

Figure 4. An eye movement sensor [18].

From the left: the sensor attached to the temple, the upper eyelid, and the lower eyelid.

2.3.2 Cardio-stimulation on a pig

Another exciting application of piezoelectric EH was presented in [19] by Bingwei Lu and his team. They designed, implanted, and assessed a PZT ultra-flexible harvester usable for harvesting energy from cardiac motions (Figure 5). This research was performed on a swine for the purpose of investigating its possible applications for medical implants such as pacemakers. An output voltage of 3 V was measured with an average voltage ranging between 2-3 V, depending on the location of the harvester. This supports the possible application as a power source for a pacemaker as lithium iodine batteries (commonly used in pacemakers) generate about 2.8V at body temperature [20]. Lu's team states possible modifications of output voltage by changing the location of the PZT implant and by specific structural changes to meet the desired needs to be used for medical devices.

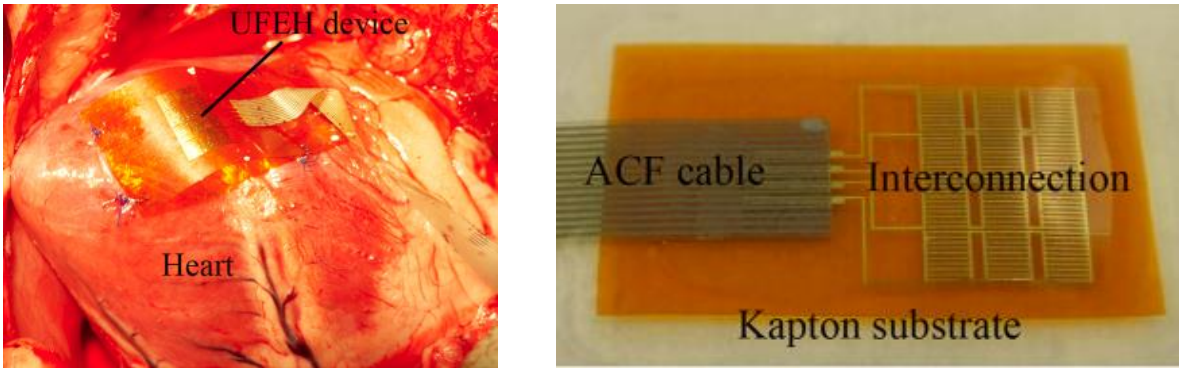

a **b**

Figure 5. A PZT UFEH for cardiac harvesting.

a - The UFEH implanted on a swine's heart, b - the PZT ultra-flexible harvester itself

2.3.3 Pacemakers

Regarding pacemakers, Medtronic, a leading firm in pacemaker development, has come up with a miniature pacemaker "Micra". Compared to a classic, robust pacemaker implanted by a wire and stimulated from an outer body power source, the Micra is a miniature device implantable intravenously through a catheter system near the upper thigh into the right ventricle of the heart. The device is then fixed against the heart wall where it functions without any external input [16]. The Micra design is visible in Figure 6.

Compared to a standard pacemaker with a life expectancy of seven to ten years [21], Medtronic estimates the battery life of Micra from eight to thirteen years [22] which is a noticeable improvement. This piezoelectric based device [23] should relieve patients of discomfort caused by a classic pacemaker.

a **b** **c**

Figure 6. Pacemakers from Micra.

a - A classic pacemaker with leads [16], b - The miniature pacemaker Micra, c - The implanted position of Micra [24].

2.3.4 Tactile sensors

A common application of piezoelectric materials and devices is in constructing tactile sensors.

W. Lin and his team of researchers from Hong Kong and Shenzhen have created [25] a skin inspired PVDF sensor array capable of, to a significant extent, mimicking the sensory properties of skin. The sensor's ability to distinguish pressure and bending real-time was proven to be also of great use for blood pressure sensing. The sensors output parameters could also be used for powering small devices, as sensed output voltages reached up to 0.9 V when bending. Even though not yet technologically advanced, this sensor brings hope for burn victims and other tactile impaired people.

Compared to other tactile sensor arrays requiring n x m wires for n x m electrodes, this sensor requires only n + m wires for n x m electrodes. Not only does this cut production costs, but it also enables connecting several sensors together. The team's sensor design, output parameters and blood pressure testing can be seen in Figure 7.

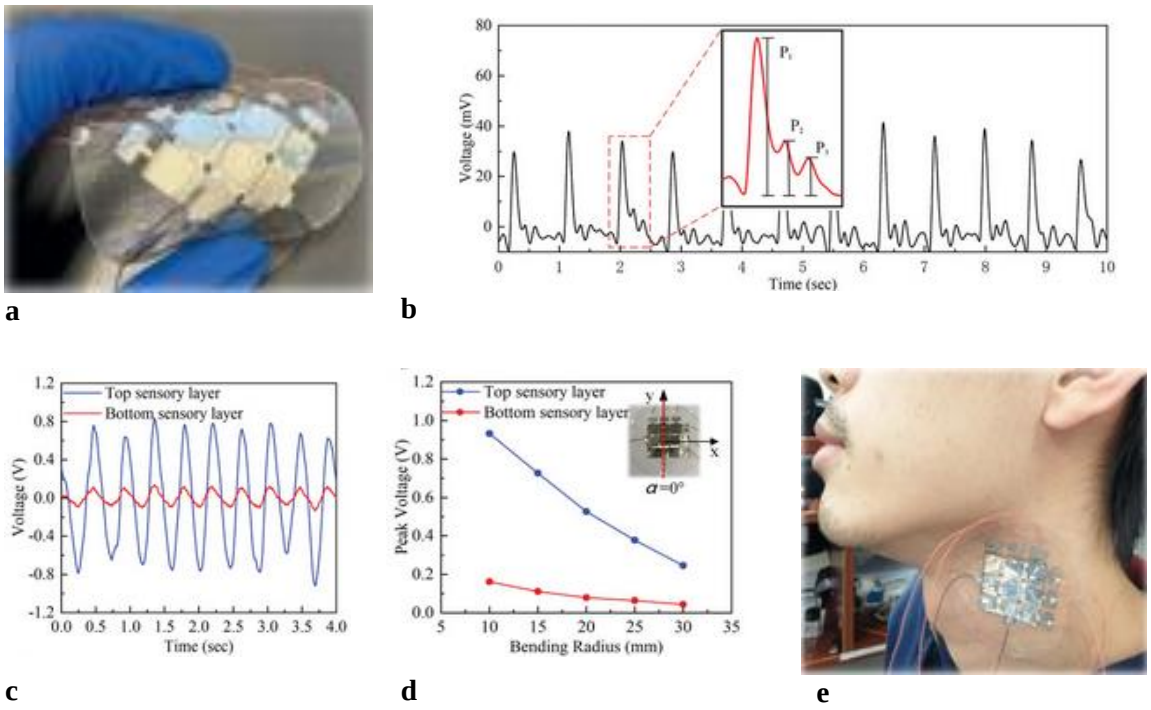

Figure 7. A tactile sensor array and its output.

a - The design of the skin inspired sensor array, b - The output voltage of blood pressure sensing visible in E, c - The output voltage from bending in the y axis, d - Bending voltage output diagram in the direction of the y axis (0º angle), d - Blood pressure sensing on a subject [25].

2.3.5 Blood pulse monitoring

An arterial blood pressure sensor based on ultrathin PZT was presented [26] by Dae Yong Park et. al. This sensor is applicable not only on the carotid and wrist arteries, but also on the throat to monitor swallowing (Figure 8A, B). The pulse sensor is connected to an amplifier circuit and a signal processing circuit. It can then be connected to a micro-controller and a Bluetooth transmitter for real-time, wireless blood pressure monitoring. Further information can be found in [26].

2.3.6 Shoe harvester model

An energy harvesting shoe was presented in [27]. The model uses as its energy source a PZT bending element and foot strike element (Figure 8C). The shoe can store energy in a capacitor, sense pressure and record data based on the physical activity of the wearer. Depending on whether the wearer walks, jumps or runs, different output and pressure layout was recorded. The devices walking output can be seen in Figure 8D. This device can be used in patient recovery monitoring or diagnosis. Even though the design is functional, it is not fully prepared for clinical use as a diagnosis tool. However, it is an efficient power source that can be adapted to power other monitoring devices and health devices.

2.3.7 Endoscopy tumour sensing

A PVDF tactile sensor used for endoscopic soft mucosal tumour detection was created by prof. Chuang and others in [17]. The sensor's working principle is evaluating the ratio of output voltages from two varyingly stiff materials, E_1 and E_2 and can be seen in Figure 9A. When sensing objects, the stiffer material E_1 produces voltage V_1 almost regardless of the object's stiffness. However, the lenient material E_2 produces varying voltage V_2, depending on the object's stiffness. The ratio $\frac{V_1}{V_2}$ then describes the stiffness of the measured object. A commending feature of this sensor is its diameter of 1.4 mm. This miniature size allows precisely locating a growth on the sensed tissue, in the case of prof. Chuang's research the submucosa of a pig stomach and artificial tumours. The sensor is also attachable to an endoscope or a catheter for obtaining real-time data (Figure 9B).

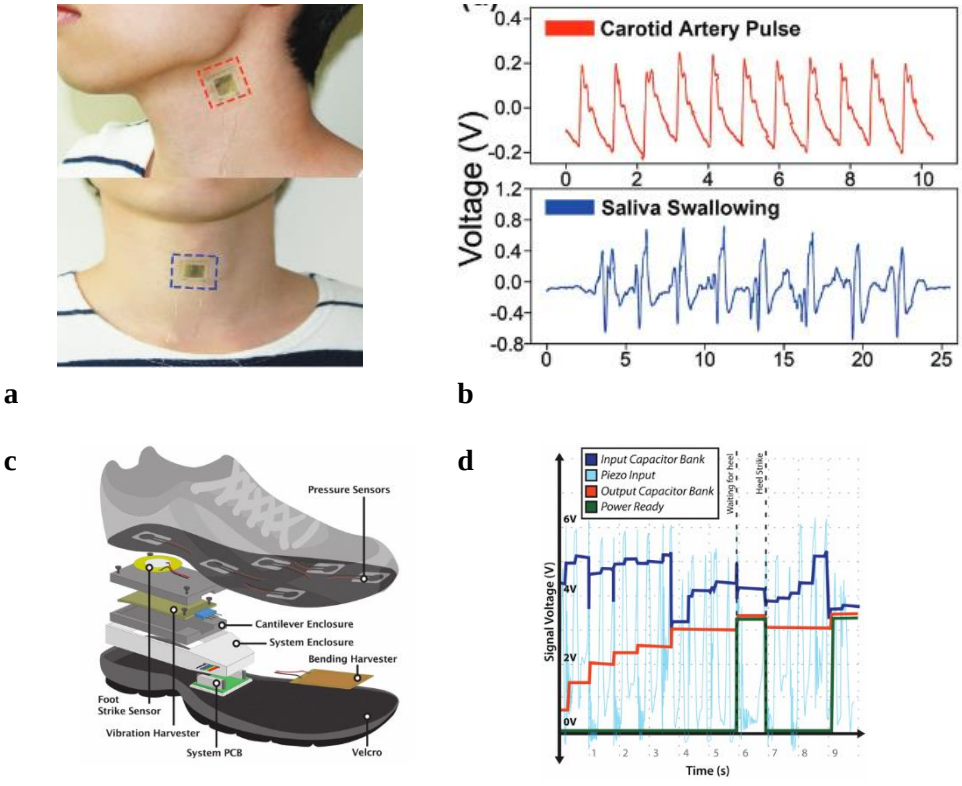

Figure 8. An arterial blood sensor and a shoe harvester model.

a - An arterial blood sensor attached to the carotid and throat, b - Voltage measured from the arterial blood sensor [26], c - A piezoelectric shoe harvester design, d - Walking voltage output from the shoe harvester [27].

2.3.8 Research for bone healing

For future research and applications, D. Khare, B. Basu and A. K. Dubey have performed a study on the possibilities of using piezoelectric materials for bone and tissue regeneration [28]. They state that similarly to piezoelectric materials, bone exhibits electrical charge when under strain. This could indicate the use of bio-compatible piezo electrics as implants for promoting bone fracture repair. Amongst other compatible piezo electric materials, authors state $BaTiO_3$, ZnO, Boron Nitride and PVDF-TrFE were all used to positively enhance bone tissue growth. With practical research being austere and mostly performed on rats, any physical model or practical application of piezo electrics in tissue healing remains for the future.

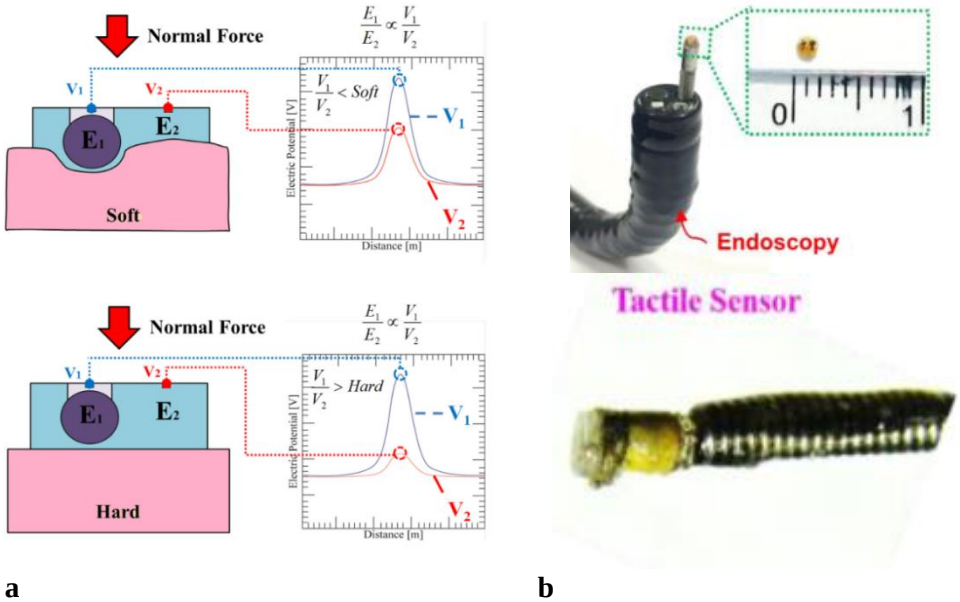

Figure 9. An endoscopic tactile sensor.

a - The working principle of the endoscopic tumour sensor, b - The sensor mounted on an endoscope and the sensor itself [17].

Chapter 3: A Piezoelectric Harvester Model

This chapter discusses my initial design of a piezoelectric energy harvester, its building steps and issues encountered designing the model and the parts of this model. After consulting with my supervisor, the work assignment is altered compared to the original assignment. Due to issues encountered discussed in Chapter 4: and this page's footnote[1], this work focuses on the output of the piezoelectric generator rather than the output of the whole model.

3.1 The model's design

My model was intended to be made up of two main parts. A piezoelectric generator and an energy harvesting circuit (Figure 10). The energy harvesting circuit has several capacitors for storing the harvested energy as well as different output modes. The circuits design is presented later (3.4). Other than these two main parts, the circuit enables further connectivity to other circuits, which I do not use, and it has output pins to which further elements can be attached.

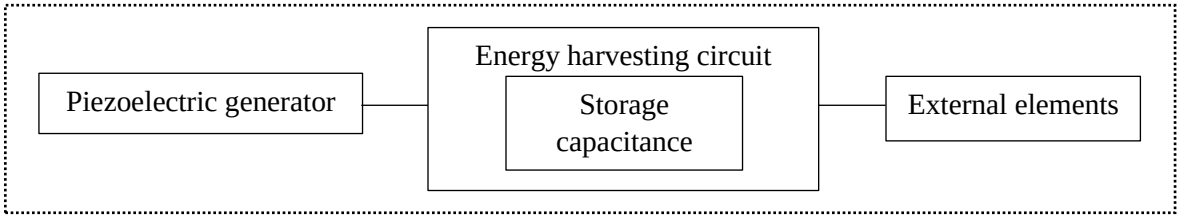

Figure 10. The block diagram of the model's design.

3.2 Building steps and issues encountered

The first step of designing this piezoelectric energy harvesting (PEH) model was finding components theoretically compatible not only with each other, but also with the human body. This proved to be one of the harder tasks as the resonant frequency of a standing human is 9 Hz to 16 Hz [29], with walking having a frequency of around 2 Hz [30] and a beating heart having a frequency of 1-2 Hz. These frequencies strictly limit my choices of a piezo generator.

I had to rely on commercially available sources, as time and finances didn't allow to create a custom piezoelectric generator. There are several distributors in the Czech Republic selling piezoelectric generators and components, the leading firms being "Farnell" and "Mouser" from which I sourced my components. I found some interesting generators such as the FS-2513P, a film beam-like piezoelectric generator, but its parameters, mainly its resonant frequency of 80 Hz [31], weren't compatible with body movements. This was also the issue with other commercially available piezoelectric generators as they had resonant frequencies even higher than 80 Hz. I ended up choosing the 10184000-01 from TE Connectivity, which is intended as a sleep monitor strip [32], to test its possibilities as an energy harvesting device. I chose this generator because of two reasons. It seemed plausible for biomedical applications not only as an energy harvester, but also as a sensory element and the datasheet listed at 0.1 Hz a voltage output of up to 70 V and a charge of up to 500 nC which both seemed high considering the low frequency. The next step was finding a suitable integrated circuit for managing and storing the harvested energy. Out of the possible options, I opted for the DC2042A by Analog Devices as it's designed for piezoelectric energy harvesting [33] and commercially available from either of the leading firms. I discovered its incompatibility with the 10184000-01 piezoelectric strip through measurements.

[1] Due to over a month's delay waiting for the delivery of the model's parts and due to discovering insufficient output parameters of the piezoelectric strip to power the energy harvesting circuit during measurements, my supervisor and I have subsided from the original assignment and are focusing on the piezoelectric generator. The steps encountered are discussed.

3.3 Piezoelectric generator 10184000-01

The 10184000-01 is a thin PVDF strip approximately 80 cm long with a width of 8 mm and thickness of around 30 µm, the piezoelectric element itself is 70 cm long and 3 mm wide [32]. Its highly flexible properties allow creating a piezoelectric charge from various positions. The manufacturer states that the strip generates charge or voltage output when subject to dynamic strain, mostly change in length [32]. These parameters have been tested in this manner and the results are presented later. The strip's application as a sleep monitor strip is also discussed. The strip can be seen in Figure 11.

a **b**

Figure 11. The 10184000-01 piezoelectric strip.

a - The piezoelectric strip, b - The piezoelectric strip in its encasing.

3.4 Integrated circuit DC2042A

The DC2042A, which I chose for harvesting energy from the piezoelectric generator, is a multi-purpose harvesting circuit created by ANALOG DEVICES. It has several selectable applications: A solar harvesting circuit marked JP4, a diode voltage drop circuit marked JP3, a thermoelectrical generator harvesting circuit marked JP2 and a piezoelectric energy harvesting circuit (Figure 12) marked JP1, which I intend to use when connecting the piezoelectric generator.

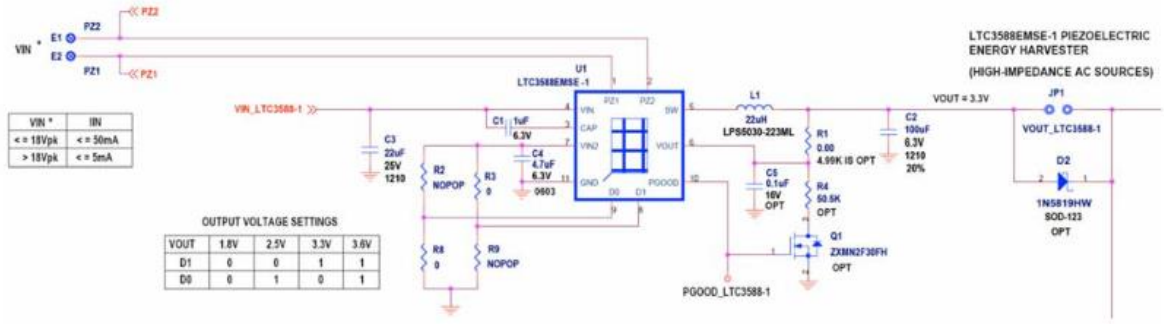

Figure 12. The schematic of the piezoelectric harvesting circuit of the DC2042A.

The basis of the circuit is an LTC3588-1 (Figure 13) by LINEAR TECHNOLOGY which consists of a bridge rectifier to rectify the input from the piezoelectric element, an UVLO, Undervoltage Lockout, which enables the Buck Converter to transfer the charge from the input capacitor to the output capacitor when the UVLO threshold is exceeded. The circuit also has a Power Good comparator (PGOOD) which keeps the output voltage V_{OUT} active until it falls to 92 % of the desired regulation and an Internal Rail Generation which drives the Buck Convertor's MOSFETs [34].

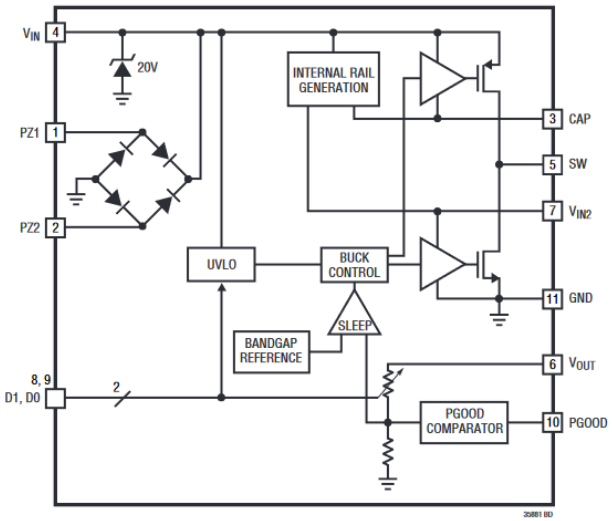

Figure 13. The design of the LTC3588-1

The basic principle of harvesting piezoelectric energy with the DC2042A (Figure 14) is this: A piezoelectric generator is attached to the PZ1 and PZ2 pins, the output of the piezo generator is rectified and stored in the input capacitor until it reaches the UVLO threshold from where it is transferred to the output capacitor and to the LTC3588-1 V_{OUT} pin which is connected to the DC2042A main V_{OUT} pin. From there we can use the stored energy by connecting to the main V_{OUT} pin and to the HGND or BGND pins. The LTC3588-1 has an input, inactive, current of 950 nA with output in regulation and input operating range of 2.7 V to 20 V [35], which needs to be reached for operating the circuit.

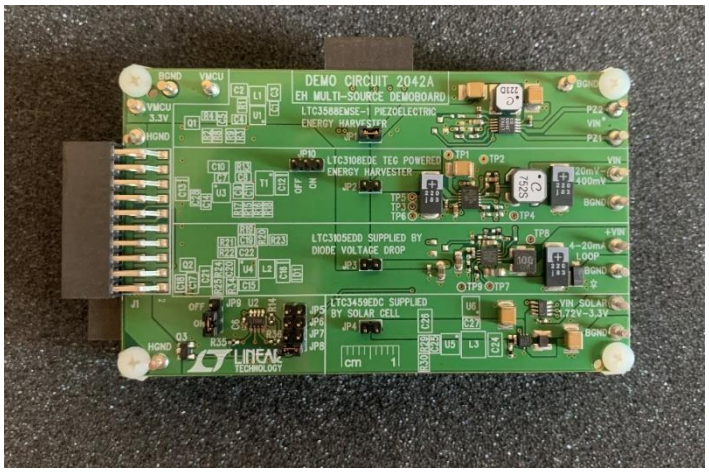

Figure 14. DC2042A.

From the top: The piezoelectric EH circuit JP1, the thermoelectrical generator harvesting circuit JP2, the diode voltage drop circuit JP3 and the solar harvesting circuit JP4.

Chapter 4: Measurements:

This chapter describes the process of measuring the model's parameters, the measured data, and the insufficiency of the piezoelectric strip to power the harvesting circuit.

4.1 Devices used:

For measurements I used these devices visible in Figure 15:

- RIGOL digital oscilloscope MSO5204 with a 200 MHz bandwidth, an 8 GSa/s sampling rate and an 8-bit resolution [36].
- PA5100 signal generator with a selectable frequency from 16 Hz higher.
- Resistance decade box with selectable resistances from 0.9 Ω to 99999 Ω with a deviation of 0.1 %.
- METEX ME-22 multimeter in its AC voltage measurement mode with a selected range of 200 mV.

Figure 15. Devices used.

From the left: RIGOL MSO5204 oscilloscope, PA5100 signal generator, Resistance decade box, METEX ME-22 multimeter

4.2 Measuring the piezoelectric generator

The first step in assessing my model was to measure the output parameters of the piezoelectric strip. For this I used the facilities of the laboratory of microelectronics in the Faculty of Electronics CTU. I would like to thank Ing. Jiří Kroutil, Ph.D. and Ing. Alexandr Laposa, Ph.D. for their assistance and advice during my measurements.

Due to the strips size, mostly its length and thickness, I opted for keeping it in its packaging consisting of a soft, thin cardboard encasing (Figure 11B) and a plastic strip on which the strip lays on the inside. This was because of two reasons. Firstly, direct measurements on the strip without knowing its approximate properties could damage it. Keeping it in a casing of sorts protects it from external damage like cuts, breaks, twisting or humidity (the strip is not entirely water resistant). Secondly, this casing mimics its manufacturers intent of a sleep monitor strip. The datasheet states the strips output parameters when placed on top of a mattress or under a mattress protector [32]. The encasing should provide similar output parameters as when placed between a mattress and a mattress protector.

The first step in measuring the generator strip was to attach it in place. I did so in two positions. The first was on two vertical rod holders (Figure 16A) and the second was on two horizontally placed rod holders (Figure 16*B*) so the piezoelectric strip could be attached to the signal generator. I attached the strip in its encasing simply with tape. I extended the manufacturers solder tabs with two pieces of insulated wire to ensure no damage would be done to the strip when manipulating with it. I then attached the wires to the oscilloscope to directly measure the strips parameters. This effectively added a 1 MΩ impedance to the output [37].

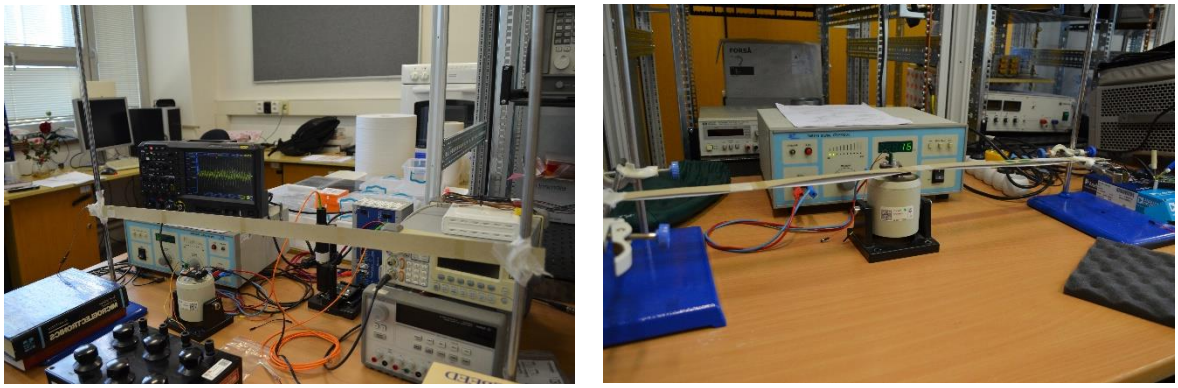

a **b**

Figure 16. The piezoelectric strip attached for measurements.

a - vertically attached piezo strip for low frequency measurements, b - horizontally attached piezo strip with the signal generator for higher frequency measurements.

4.2.1 Low frequency data

My measurements were divided into two parts. The first part was to establish the strips output at low frequencies (attachment on Figure 16A). Unfortunately, I encountered a significant problem. The laboratory did not have a low frequency source. I had to create the impulses by hand, leading to each measurement having a different impulse amplitude. This also created a slight recoil in the strip, and some resounds, mostly visible in the spectra. However, it sufficed to acquire the output voltages and the power of these signals at these low frequencies. I recorded the data with the oscilloscope and used MATLAB to plot out the signals and the spectra. The power of these signals was calculated using the root-mean-squared to the second power (RMS^2) of each signal, all calculated in MATLAB. The power of each sample signal can be seen in Table 2. A sample low frequency signal and its spectrum can be seen in Figure 17. The power of each signal is unfortunately not relatable to every signal, as the impulse amplitude deviation was not stable, mostly in the ranges of 1-2 cm and the time of the first peak is not consistent throughout the signals. Even though single measurements provide a good insight to the response of the piezoelectric strip, they don't describe a precise relationship between total power and frequency. However, the knowledge of peak-to-peak (p-p) voltages, currents and powers is important in deciding whether the strip can power the harvesting circuit.

I also attached the resistance decade box at different resistance settings to the piezo strip parallel with the oscillator to see how the output voltages differ. A significant decrease was seen at both 1 Hz and 2 Hz with larger decreases seen on lower attached resistances (Attachments a-d). I also wanted to measure the output current of the strip, but the current was too low for the multimeter to read, and I didn't dispose of any better current measuring device. I calculated the total average current output from the knowledge of the oscilloscope's impedance and the signal's total power as:

$$I = \pm\sqrt{\frac{P}{Z}} \tag{19}$$

Where I is the average current, P is the signals total power and Z is the impedance of the total load.

I estimated the p-p voltages and currents from the signals. From these I calculated the p-p powers. The low frequency signal currents, and p-p parameters can be seen in Table 2.

a

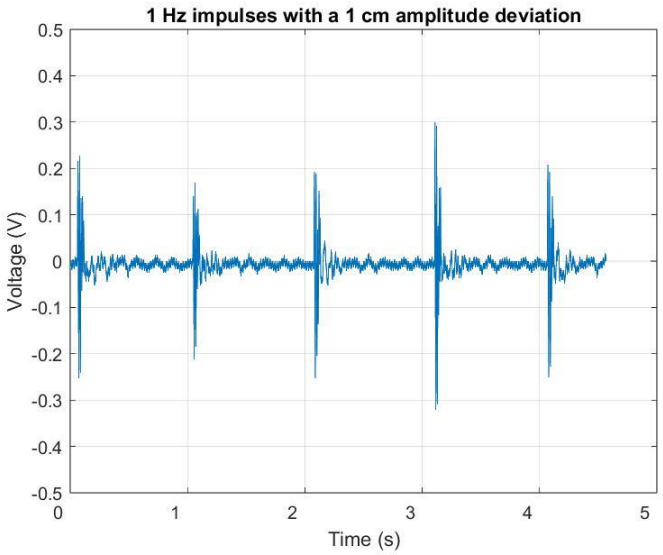

b

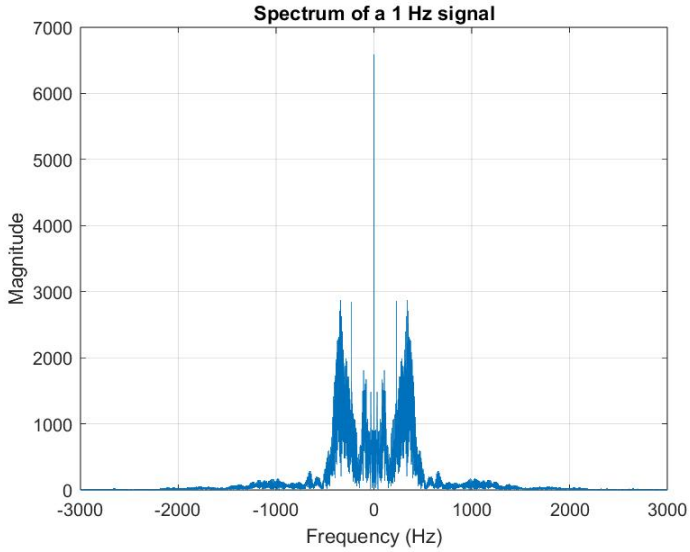

Figure 17. A sample 1 Hz voltage output.

a - The 1 Hz voltage wave, b - The spectrum of the 1 Hz voltage output.

Table 2. Low frequency output acquired from measured voltage signals.

Frequency (Hz)	1	1	2	2	2	3	4	4.75	5.25
Approx. amplitude (cm)	1	1	1	1	1	1.5	2	1.5	2
Resistance added (kΩ)	-	100	-	20	50	-	-	-	-
Total impedance (kΩ)	1000	99	1000	19.6	47.6	1000	1000	1000	1000
Power (µW)	1100	160	-	78.7	137.4	3500	14200	5300	8200
Approx. sample time (s)	4.5	5	5	5	4.6	4.8	5	4.7	4.7
Current (µA)	33.2	12.7	-	8.9	11.7	59.6	119.4	73.0	90.7
Peak-to-peak Voltage (V)	0.6	0.2	0.56	0.08	0.15	0.7	1	0.7	0.95
Peak-to-Peak Current (µA)	0.6	2.02	0.56	4.1	3.15	0.7	1	0.7	0.95
Peak-to-Peak Power (nW)	360	404	314	410	473	490	1000	490	903

4.2.2 Higher frequency data

The next part was to establish the strips higher frequency response. I did so in a similar manner as with the lower frequency measurements. The measurement setup can be seen in Figure 16B. These measurements were more precise compared to the lower frequency measurements as I had the signal generator to vibrate the piezo strip. The main difference is visible in the spectra of these signals, as the higher frequency signals have clear and discrete harmonics (Figure 19 compared to Figure 17).

I also measured the strips voltage output using only the multimeter in its AC Voltage, 200 mV setting to get a sense of how the strip responds on varying frequencies. I generated frequencies from 16 Hz to 48 Hz with the signal generator and looked at some low frequency impulses when striking the piezo strip by hand. These low frequencies weren't properly recordable as I didn't know the exact impulse frequency and the voltage on the multimeter fluctuated too much. I however saw measured voltages above 100 mV when applying single digit frequencies which would support the rising trend of the voltages from 20 Hz to 15 Hz visible in Figure 18, created with [38]. Out of these measurements, the highest output voltage of 98.6 mV was recorded on 21 Hz. This could indicate that 21 Hz is a resonant frequency. However, given the p-p voltages recorded with the oscilloscope in Table 2 and Table 3 and the exponential approximation mimicking the decrease of the 15-20 Hz data in Figure 18, only 80 mV shifted, I incline to the possibility of recording flukes from 20 Hz lower. The multimeter may not be capable of precisely recording frequencies lower than 20 Hz (I wasn't able to find the multimeter's parameters). Given the unknown variables, I chose to disregard these data in the approximation.

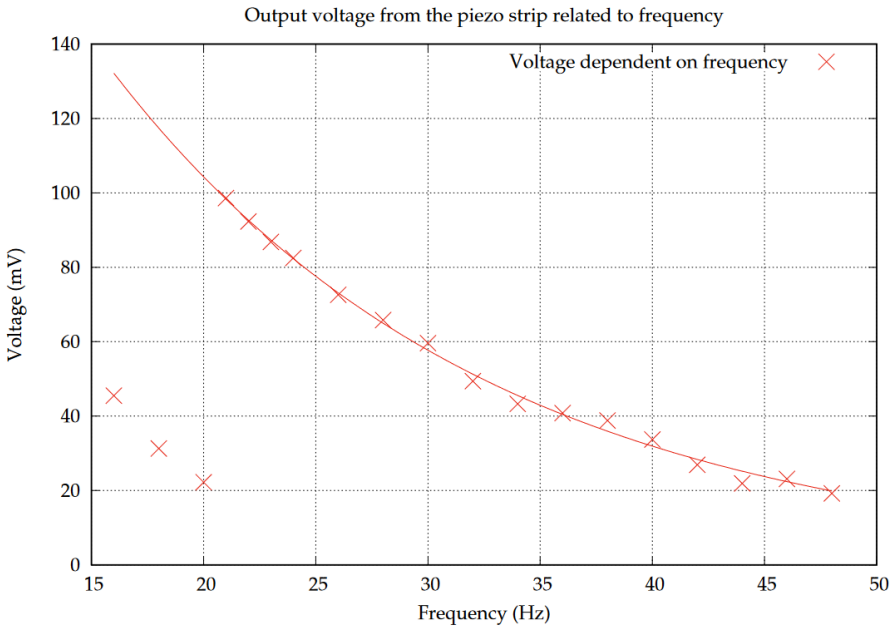

Figure 18. A graph of measured voltage dependent on frequency approximated by an exponential function.

$V(x) = A \cdot e^{kx}$, *A = 340.85373026198, k = -0.059202743400401.*

As with the low frequency signals, I calculated the power using RMS^2 of each higher frequency signal. I also estimated the average current using (19) and calculated the peak-to-peak voltages, currents, and powers from each signal, visible in Table 3. The impulse amplitude was around 1 cm.

a

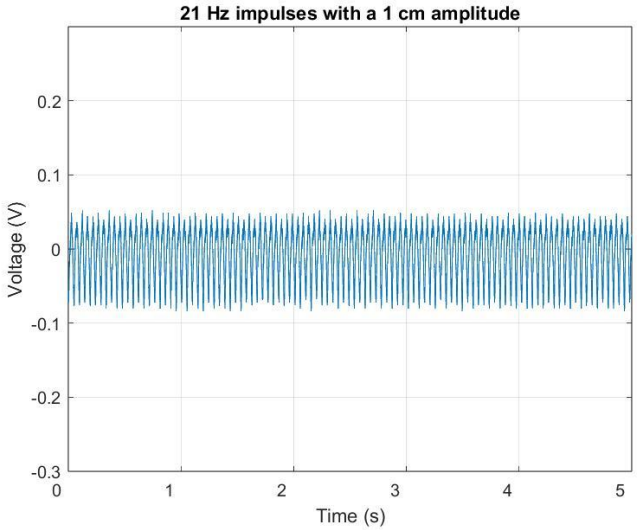

b

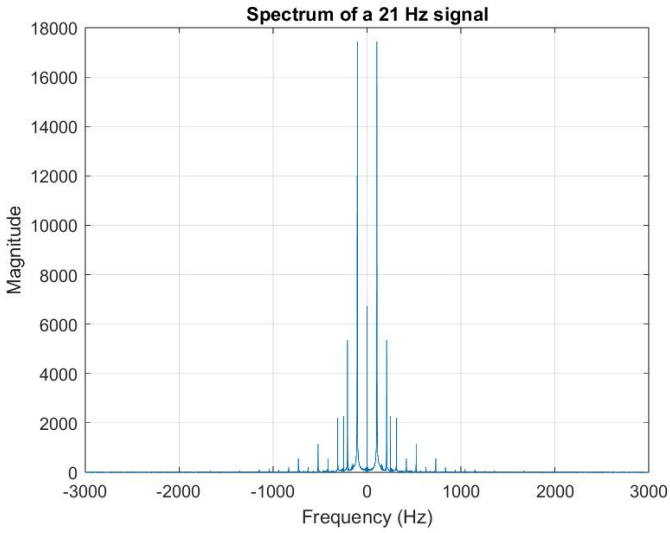

Figure 19. A sample 21 Hz voltage output.

a – The 21 Hz voltage wave, b - The spectrum of the 21 Hz voltage output.

Table 3. Higher frequency output acquired from measured voltage signals.

Frequency (Hz)	16	21	24	32
Resistance added (kΩ)	-	-	-	-
Total impedance (kΩ)	1000	1000	1000	1000
Power (μW)	1500	1247	658	8200
Approx. sample time (s)	5	5	4.9	4.7
Current (μA)	38.7	35.3	25.7	39.7
Peak-to-peak Voltage (V)	0.20	0.12	0.09	0.16
Peak-to-Peak Current (μA)	0.20	0.12	0.09	0.16
Peak-to-Peak Power (nW)	40	14.4	9	25.6

4.2.3 Peak-to-Peak voltage

An interesting output from my measurements was the p-p voltage to frequency dependency. To achieve this dependency, I had to modify my output values as if they were created by the same impulse amplitude of 1 cm. I did so by dividing them by their amplitude. I divided the 3 Hz p-p voltage by 1.35 as to 1.5 as a correction factor, as the signal's overall peaks weren't as high as the 4.75 Hz signal which had a 1.5 cm amplitude. This created the graph in Figure 20 using [38] (Blue points coincide with red points). I used two different approximation functions. I did this because I don't have any data between 6 Hz and 15 Hz and also because the p-p value of 32 Hz seemed too high. Disregarding the 32 Hz value from the exponential approximation created a well-fitting curve. The reader may have noticed the similarity of exponential approximations in Figure 18 and Figure 20. Although they have similar trends, I am unable to combine these measurements, as I do not know the load of the multimeter used to measure the data in Figure 18.

I allowed myself to convert the voltages to the same impulse amplitude, as the difference between bending from a 1 cm amplitude (≈1.6 %) and bending from a 2 cm amplitude (≈3.2 %) doesn't affect the linearity of the output voltages as significantly as higher amplitudes do (4 cm is ≈6.4 %, 10 cm is ≈16.1 %).

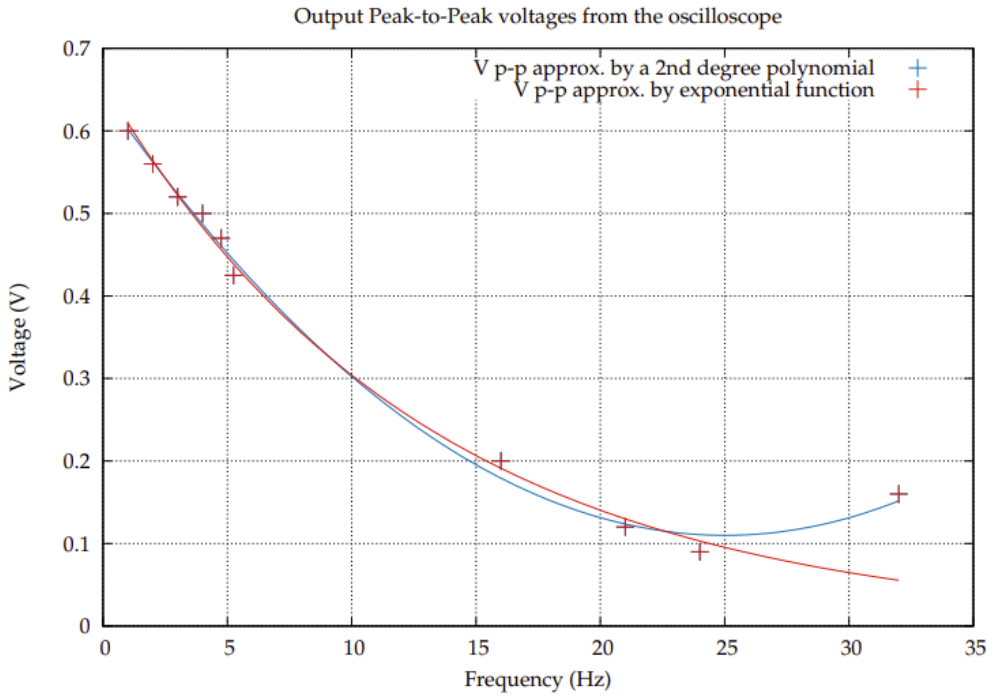

Figure 20. Peak-to-Peak voltage to frequency dependency estimated from measured data.

The red curve estimation: $V(x) = A \cdot e^{kx}$, $A = 0.65827996092985$, $k = -0.077253809532202$.
The blue curve estimation: $V(x) = a_0 + a_1 x + a_2 x^2$, $a_0 = 0.64428113216533$, $a_1 = -0.042734112403791$, $a_2 = 0.00085445375399908$.

4.2.4 Peak-to-Peak power

In order to power the DC2042A PEH circuit the piezoelectric strip would have to produce power of at least 2565 nW. When constricting myself to impulse amplitudes around 2 cm, I wasn't close enough to this value. I would need a further 1600 nW of power to reach this threshold. Using the same conversion as in 4.2.3, I got output p-p powers for 1 cm impulse amplitudes and plotted the values using MATLAB. They are visible in Figure 21. Apart from the highest value of 500 nW on 4 Hz, we can see a falling trend when we increase the frequency of the signal. Another interesting thing is the power difference between loads on the 1 Hz and 2 Hz data. On both these frequencies the p-p power is higher when lower loads were applied. This could be a trait of the piezo strip, but as I didn't measure the low frequency data on precisely the same impulse amplitudes, I conclude that it describes the power difference between each sample. This would mean that the true value of the piezo strips power on 1 and 2 Hz is slightly higher than measured.

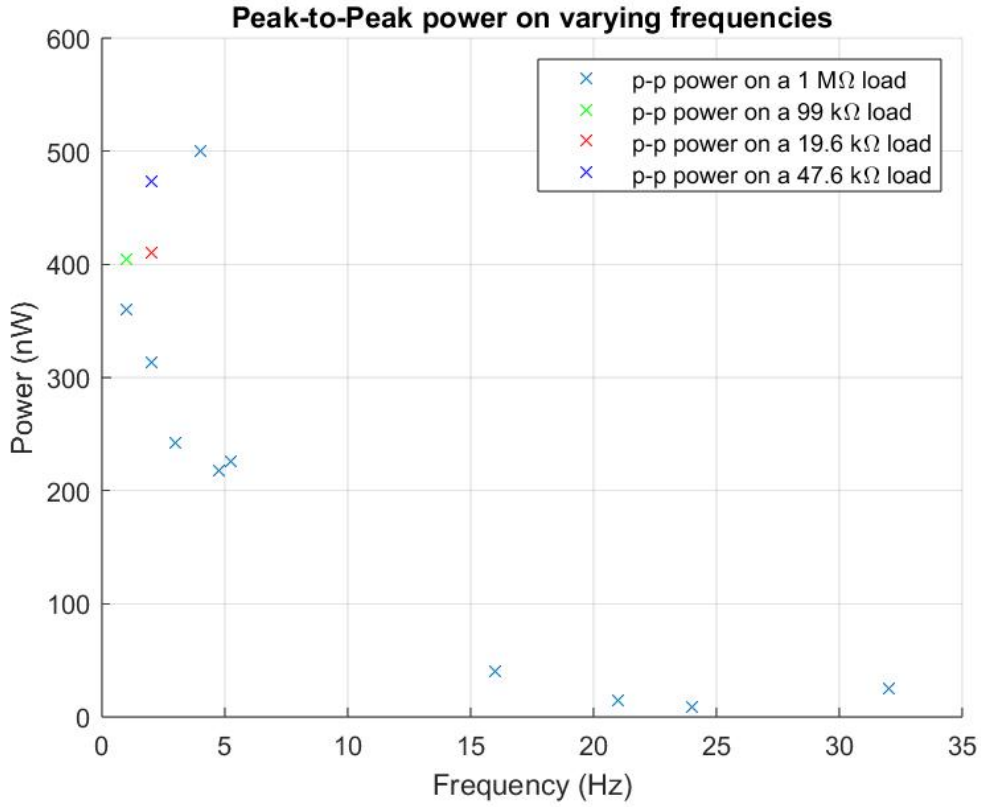

Figure 21. Peak-to-Peak power from sample measurements approximately converted to 1 cm impulse amplitude deviations

4.2.5 The piezo strip as a sleep monitor

As a matter of interest, rather than research, I tested the sensing capabilities of the strip in its manufacturer's intent as a sleep monitor. I put the strip in its encasing as well as outside of it on an inflatable mattress and attached it to the oscilloscope. I then laid on the mattress on the strip and also on the mattress under the strip with the strip laying on my abdomen and on my chest. I couldn't record any of my vitals even though gentle tapping on the piezo strip generated recordable signals. I was surprised by the sensitivity of the strip as this tapping was clearly visible on the oscilloscope. This sensitivity was also visible on the close-up of the higher frequency signals (Figure 22). I think that using this strip as a sleep monitor would need further amplification as well as some signal processing to filtrate the desired output like heart rate and breathing.

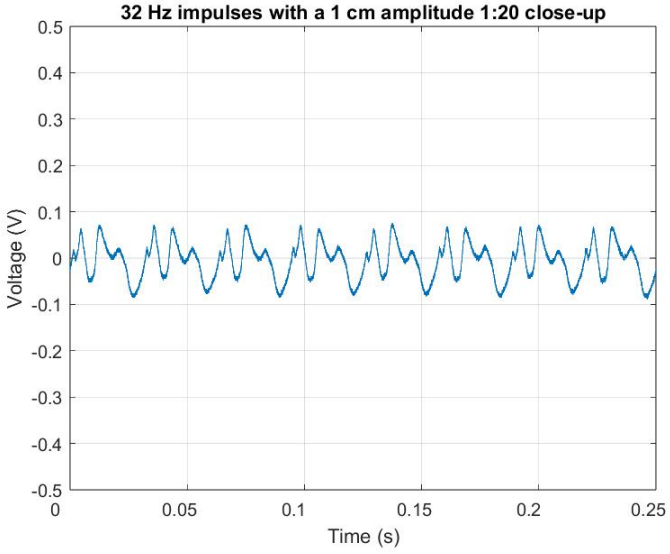

Figure 22. A close-up of a 32 Hz signal to show the sensitivity of the piezo strip.

4.3 Summary

The strips highest peak-to-peak voltage of 1 V and peak-to-peak current of 1 µA were recorded at 4 Hz with an impulse amplitude deviation of around 2 cm. This 4 Hz signal and a 16 Hz signal can be seen in Attachments e-f. These p-p parameters were achieved at a 1 MΩ impedance load with voltage peaks decreasing when lowering the load down to 19.6 kΩ. Although not a general parameter, the most powerful output was also achieved at 4 Hz. Overall, the output of the piezo strip is dependent on the amplitude of the impulses and the load attached, with higher voltage output achieved on loads of 1 MΩ and higher current output achieved on 19.6 kΩ both on impulse amplitudes higher than 1 cm. Taking these parameters into account, the piezo strip itself is not sufficient to power the DC2042A piezoelectric harvesting circuit. It can reach sufficient current output on a 1 MΩ load, but its peak-to-peak voltage output is not high enough to satisfy the circuit's needs. If I were to increase the load on the piezo strip, I could achieve higher voltages, but the peak-to-peak current would decrease below the 950 nA threshold leading to the inoperability of the circuit. Increasing the impulse amplitude to a maximum at a load slightly lower than 1 MΩ may result in higher, even sufficient peak-to-peak outputs, but as I tested the strips application as a biomedical EH power source, these tests would be inconclusive, because the average human body doesn't have an 80 cm long surface capable of creating frequent, above 10 cm amplitude deviations.

4.4 Measuring with the DC2042A:

Another part of testing my model design was connecting the strip to the piezoelectric harvesting circuit and measuring its output parameters. Due to aforementioned reasons, this chapter has no concrete output and only describes trying to achieve an output from the whole model.

4.4.1 Initial measuring

Directly after measuring the piezoelectric strips parameters, I tried attaching the strip to the piezoelectric harvesting circuit. The first step was to "select" the PEH circuit by installing the JP1 pin. I then attached the piezo strip to the PZ1 and PZ2 pins and the oscilloscope to the V_{OUT} pin (marked VMCU or VMCU 3.3 V). Without having the piezo strips output parameters calculated yet, this was solely a test whether the whole model is functional itself. At this time, I did not know of the 2.7 V low threshold and the 950 nA inactive input current threshold of the LTC3588-1 sub-circuit as it wasn't stated in the DC2042A datasheet (I found out about it after searching for it after these measurements). These initial tests were a failure.

Not recording any output made me think that the 1 MΩ load of the oscilloscope was too high for the circuit and that it was stopping any current flowing to the oscilloscope. This led me to change the output to the multimeter which would put a lower load on the circuit, increasing the current. I was able to get some small readings rising from tenths of mV up to higher single digit mV when really straining the piezo strip, but they seemed more like flukes rather than legitimate readings.

At this point, I realised that the problem was probably with the piezoelectric strip, so I tried adding some resistance between the strip and the PZ1 and PZ2 pins. This would increase the voltage to the circuit, but I recorded no change. I then abandoned further tries and proceeded with evaluating the measured signals and investigated the parameters of the circuit. This eventually led me to the conclusion that the piezoelectric strip isn't suitable for the DC2042A PEH harvesting circuit.

Chapter 5: Further progress and upgrades

This chapter thinks upon further applications of the piezoelectric strip and possible upgrades to the model.

The biggest downside of this model is the discovered incompatibility of the 10184000-01 piezoelectric strip with the DC2042A PEH circuit in its "plain" state. The simplest solution to this problem would be to replace the 10184000-01 with another, most probably not as biomedicinally suitable, piezoelectric generator (such as the FS-2513P). This should create sufficient parameters to operate the circuit. However, it may not be applicable as a body-sourced biomedical harvester due to its high resonant frequency. Another possible solution would be to amplify the piezoelectric strip by adding an externally powered element to the circuit, such as an operational amplifier. The question is whether the elements power demand wouldn't exceed the strips output capabilities, making the principle obsolete. One more possible modification would be to design the strip with a different piezoelectric material such as PZT, as PZT has much higher d_{33} and k values leading to higher charge outputs. The limiting factor of doing this would be the maximum flexibility of the strip because PZT isn't as flexible as PVDF. At this piezoelectric length of 70 cm, the strip could break even under its own weight as PZT has over 4 times the density of PVDF (Table 1).

If one would want to keep the strip unaffected, they would have to design a similar harvesting circuit to the DC2042A but decrease the input operational thresholds to around 1V and 500 nA for the strip to stably supply the circuit without the need of large deformations.

Outside of using the strip as an energy source, I would recommend the strip as a sensory element. Throughout measurements, the strip proved to be sensitive to minute vibrations and its size and flexibility should allow for uses such as the intended sleep monitor. Another possible application would be as a heart rate or respiratory rate monitor. To accomplish this, an amplifier circuit would have to be constructed as well as some signal processing to filter out the desired signals.

Out of its encasing, the strip wasn't the easiest to handle as its length made the strip twist when adjusting its position. Its thickness of 30 μm made me hesitant to strain it without the encasing as I had only one strip available. A crack in the piezoelectric film would decrease its output parameters. I wouldn't recommend using the strip without some external protection other than the piezoelectric layer protection.

Chapter 6: Conclusion

This thesis has handled designing and testing a piezoelectric energy harvesting model, testing a low frequency piezoelectric strip as its power source. For this I familiarised the reader with piezoelectric properties and principles and presented various innovations in piezoelectrically power biomedical devices. I described the process of designing this model from commercially available components and debated the theoretical compatibility of these components with the human body. I also described the process of measuring the strips parameters in order to investigate its powering capabilities. These tests showed that the strip is not powerful enough to power up the energy harvesting circuit when subject to impulses in body-compatible frequency ranges and amplitudes. By body-compatible I mean impulses that our bodies could create or comfortably endure, numerically 1-32 Hz and 1-2 cm.

Because of this discovery and over a month's delay waiting for the components, this thesis is impoverished of the results from measuring the whole model. This thesis also stated possible modifications to enhance and put the model into operation. However, some of these modifications would disregard the model's biocompatibility or autonomy as an energy harvesting model.

Creating this thesis, I stumbled into several issues. The limited market for biocompatible piezoelectric generators and harvesting circuits and the discovered insufficiency of the 10184000-01 to power my proposed model proved to be the trickiest. I however believe that I managed to handle these issues accordingly to the given time.

References

[1] PROF. MGR. JIŘÍ, Erhart, Ph.D. Piezoelectricity and ferroelectricity Phenomena and properties. In: *Dokumen.tips* [online]. Technical University of Liberec, 2010 [cit. 2023-04-25]. Available from: https://dokumen.tips/documents/piezoelectricity-and-ferroelectricity-phenomena-and-piezoelectricity-and-ferroelectricity.html?page=1

[2] PROF. ING. MIROSLAV, Husák, CSc. Autonomní mikronapájecí zdroje s piezoelektrickým principem - I. *DPS*. 2013, **1**(1), 2-4.

[3] UCHINO, Kenji. The development of piezoelectric materials and the new perspective. In: *Advanced Piezoelectric Materials: Science and Technology*. 2010, 1-7,22. ISBN 9781845695347.doi:10.1533/9781845699758.1

[4] *Polarization* [online]. Massachusetts Institute of Technology: Markus Zahn, 2021 [cit. 19.02.2023]. Available from: https://eng.libretexts.org/Bookshelves/Electrical_Engineering/Electro-Optics/Electromagnetic_Field_Theory%3A_A_Problem_Solving_Approach_(Zahn)/03%3A_Polarization_and_Conduction/3.01%3A_Polarization

[5] doc. Ing. Vítězslav Pankrác, CSc. *Pomocné texty k přednáškám z teorie elektromagnetického pole*. ČVUT Praha, 2013, 29-33 s. Study text. Czech Technical University in Prague.

[6] *Calculating Piezoelectric Material Properties from Material Datasheet* [online]. support.onscale: Cyprien Rusu, 2020 [cit. 17.02.2023]. Available from: https://support.onscale.com/hc/en-us/articles/360002073378-Calculating-Piezoelectric-Material-Properties-from-Material-Datasheet?fbclid=IwAR3sICrotu6gxdlqYRYDC_h-B7HQwI9OfQLRqei7ndQFxPJVVfVb-TzIdGk

[7] Piezoelectric mathematical modeling; technological feasibility in the generation and storage of electric charge. *IOPscience - Journal of Physics: Conference Series*. 2021, **2159**, 2. Available from: doi:10.1088/1742-6596/2159/1/012009

[8] *Piezoelectric Transducer* [online]. electricbaba.com: Site administrator, 2020 [cit. 05.04.2023]. Available from: https://electricalbaba.com/piezoelectric-transducer/

[9] NIU, Qianqian, Haifeng WEI, Benjamin HSIAO a Yaopeng ZHANG. Biodegradable silk fibroin-based bio-piezoelectric/triboelectric nanogenerators as self-powered electronic devices. *Nano Energy*. 2022, **96**, 107101. ISSN 2211-2855. doi:https://doi.org/10.1016/j.nanoen.2022.107101

[10] BOUKABACHE, Hamza, Christophe ESCRIBA a Jean-Yves FOURNIOLS. Toward Smart Aerospace Structures: Design of a Piezoelectric Sensor and Its Analog Interface for Flaw Detection: Design of a Piezoelectric Sensor and Its Analog Interface for Flaw Detection. *Sensors*. 2014, **14**(1), 6. doi:10.3390/s141120543

[11] *Ceramic Materials* [online]. bostonpiezooptics.com: various suppliers, ., [cit. 2023-04-27]. Available from: https://www.bostonpiezooptics.com/ceramic-materials-pzt

[12] RIBEIRO, Alexandre, R. MARQUES, Guastaldi CARLOS a João CAMPOS. Hydroxyapatite deposition study through polymeric process on commercially pure Ti surfaces modified by laser beam irradiation. *Journal of Materials Science*. 2009, **44**, 4059. doi:10.1007/s10853-009-3585-6

[13] SABER, Nasser, Qingshi MENG, Hung-Yao HSU, Sang-Heon LEE, Hsu-Chiang KUAN, Donavan MARNEY, Nobuyuki KAWASHIMA a Jun MA. Smart thin-film piezoelectric composite sensors based on high lead zirconate titanate content. *Structural Health Monitoring*. SAGE Publications, 2014, **14**(3), 214-227. ISSN 1475-9217. doi:10.1177/1475921714560075

[14] TAI, C.W., K.Z. BABA-KISHI a K.H. WONG. Microtexture characterization of PZT ceramics and thin films by electron microscopy. *Micron*. 2002, **33**(6), 584. ISSN 0968-4328. doi:https://doi.org/10.1016/S0968-4328(02)00016-1

[15] *How do piezo motors work?* [online]. xeryon.com: Xeryon, 2019 [cit. 2023-04-28]. Available from: https://xeryon.com/technology/how-do-piezo-motors-work/

[16] *Micra brochure* [online]. europe.medtronic.com: Medtronic, 2018 [cit. 2023-04-28]. Available from: https://europe.medtronic.com/content/dam/medtronic-com/xd-en/hcp/documents/micra-physician-brochure.pdf

[17] CHUANG, Cheng-Hsin, Tsan-Hsiu LI, I-Chinms CHOU a Ying-Juimr TENG. Piezoelectric tactile sensor for submucosal tumor detection in endoscopy. *Sensors and Actuators A: Physical*. 2016, **244**, 299-309. ISSN 0924-4247. doi:https://doi.org/10.1016/j.sna.2016.04.020

[18] KIM, Nam-In, Jie CHEN, Weijie WANG et al. Highly-Sensitive Skin-Attachable Eye-Movement Sensor Using Flexible Nonhazardous Piezoelectric Thin Film. *Advanced Functional Materials*. 2021, **31**, 2008242.doi:10.1002/adfm.202008242

[19] LU, Bingwei, Ying CHEN, Dapeng OU et al. Ultra-flexible Piezoelectric Devices Integrated with Heart to Harvest the Biomechanical Energy. *Scientific Reports*. 2015, **5**, 16065. doi:10.1038/srep16065

[20] *Pacemaker Technology* [online]. CARDIOLOGY: drzezo, 2016 [cit. 2023-04-28]. Available from: https://thoracickey.com/pacemaker-technology/#:~:text=The%20ideal%20pacemaker%20battery%20should%20be%20able%20to,also%20should%20be%20capable%20of%20being%20sealed%20hermetically.

[21] *What is the typical lifetime of a pacemaker?* [online]. London Heart Clinic: Dr Syed Ahsan, 2021 [cit. 2023-03-13]. Available from: https://theheartclinic.london/treatments/pacemakers/answerpack/pacemakers-icds/pacemakers-icds-faq/what-is-the-typical-lifetime-of-a-pacemaker/

[22] *Longevity Micra* [online]. heartbeatdoctor.com: Medtronic, 2020 [cit. 2023-04-28]. Available from: https://heartbeatdoctor.com/wp-content/uploads/2021/05/micra-physician-portfolio-brochure.pdf

[23] *Piezo in Micra* [online]. europe.medtronic.com: Medtronic, 2022 [cit. 2023-03-25]. Available from: https://europe.medtronic.com/xd-en/transforming-healthcare/EUreka/innovation-articles/energy-harvesting.html

[24] *AV synchronous pacing using a single chamber leadless pacemaker* [online]. medtronic.com: Assoc.-Prof. Clemens Steinwender, MD, FESC, 2020 [cit. 2023-04-28]. Available from: https://europe.medtronic.com/content/dam/medtronic-com/xd-en/hcp/documents/digitalhub/ehra-2020/Medtronic_Session2_Brady%20Pacing_Talk3_Steinwender.pdf

[25] LIN, Weikang, Biao WANG, Guoxiang PENG, Yao SHAN, Hong HU a Zhengbao YANG. Skin-Inspired Piezoelectric Tactile Sensor Array with Crosstalk-Free Row+Column Electrodes for Spatiotemporally Distinguishing Diverse Stimuli. *Advanced Science*. 2021, **8**, 2002817. doi:10.1002/advs.202002817

[26] PARK, Dae, Daniel JOE, Dong KIM et al. Self-Powered Real-Time Arterial Pulse Monitoring Using Ultrathin Epidermal Piezoelectric Sensors. *Advanced materials (Deerfield Beach, Fla.)*. 2017, **29**. doi:10.1002/adma.201702308

[27] MEIER, R., N. KELLY, O. ALMOG a P. CHIANG. A piezoelectric energy-harvesting shoe system for podiatric sensing. In: *2014 36th Annual International Conference of the IEEE Engineering in Medicine and Biology Society*. 2014, s. 622-625. ISSN 1558-4615. doi:10.1109/EMBC.2014.6943668

[28] KHARE, Deepak, Bikramjit BASU a Ashutosh DUBEY. Electrical stimulation and piezoelectric biomaterials for bone tissue engineering applications. *Biomaterials*. 2020, **258**, 120280. ISSN 0142-9612. Available from: doi:https://doi.org/10.1016/j.biomaterials.2020.120280

[29] RANDALL, J, R MATTHEWS a M STILES. Resonant frequencies of standing humans. *Ergonomics*. Bio-Engineering Division, Silsoe Research Institute, Bedford, UK, 1997, **40**(9), 879-886. ISSN 0014-0139. doi:10.1080/001401397187711

[30] PACHI, A. a Tianjian JI. Frequency and velocity of people walking. *The structural engineer*. 2005, **83**(-), Abstract.

[31] *FS-2513P* [online]. farnell.com: Midas sensors, 1998 [cit. 2023-04-30]. Available from: https://www.farnell.com/datasheets/3094325.pdf

[32] *Sleep monitor strip datasheet* [online]. Measurement Specialties: TE Connectivity Ltd., 2019 [cit. 2023-04-30]. Available from: https://www.te.com/commerce/DocumentDelivery/DDEController?Action=showdoc&DocId=Specification+Or+Standard%7FSleep_Monitor_Strip_Aplication_Notes_en%7FA%7Fpdf%7FEnglish%7FENG_SS_Sleep_Monitor_Strip_Aplication_Notes_en_A.pdf%7F10184000-01

[33] *IO circuit datasheet* [online]. Milpitas CA.: Linear Technology Corporation, 2004 [cit. 2023-04-30]. Available from: https://www.analog.com/media/en/technical-documentation/user-guides/DC2042AF.PDF

[34] *LTC3588-1* [online]. Milpitas CA: LINEAR TECHNOLOGY corp., 2010 [cit. 2023-05-08]. Available from: https://www.analog.com/media/en/technical-documentation/data-sheets/35881fc.pdf

[35] *LTC3588-1 product info* [online]. Milpitas CA: LINEAR TECHNOLOGY corp., 2023 [cit. 2023-05-09]. Available from: https://www.analog.com/en/products/ltc3588-1.html#product-samplebuy

[36] *Rigol datasheet* [online]. rigol.com: RIGOL technologies co., 2020 [cit. 2023-05-07]. Available from: https://rigolshop.eu/product-oscilloscope-mso5000-mso5204.html

[37] *Rigol manual* [online]. rigol.com: RIGOL technologies co., 2018 [cit. 2023-05-07]. Available from: https://www.batterfly.com/PDF/RIGOL/mso5000/MSO5000_UserGuide_EN.pdf

[38] *Planck* [online]. CTU in Prague: Milan Červenka, - [cit. 2023-05-08]. Available from: https://planck.fel.cvut.cz/praktikum/grafy/grafy.php

Attachments

a

b

a – *1 Hz data with a 1 MΩ load measured with RIGOL MSO5204,* **b** *– 1 Hz data with a 100 kΩ load measured with RIGOL MSO5204.*

c

d

c – *2* *Hz data with a 1 MΩ load measured with RIGOL MSO5204,* **d** *– 2 Hz data with a 19.6 kΩ load measured with RIGOL MSO5204.*

e

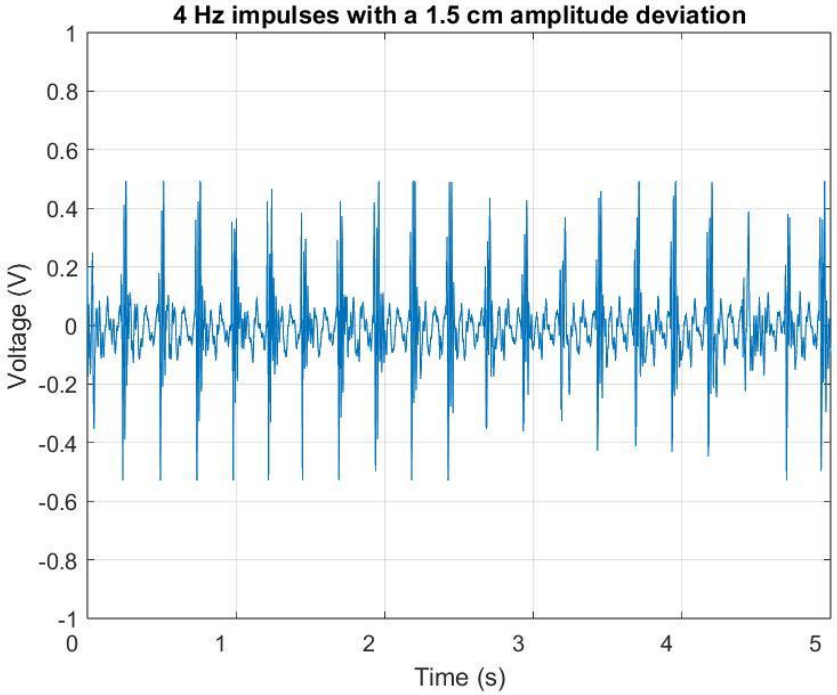

e – *A 4 Hz voltage signal wave*

f

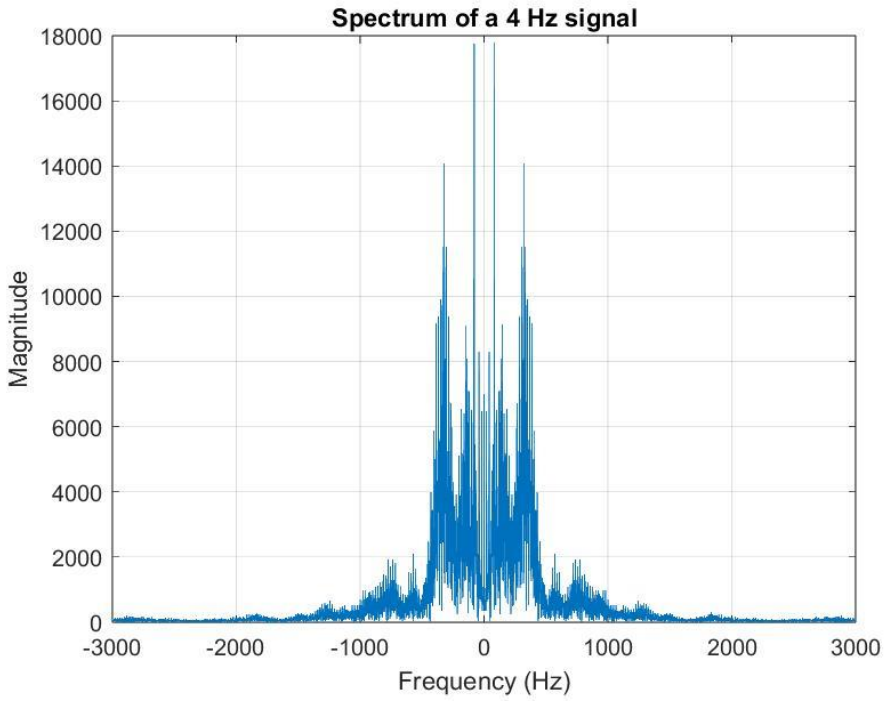

f – *A 4 Hz voltage signal spectrum*

g

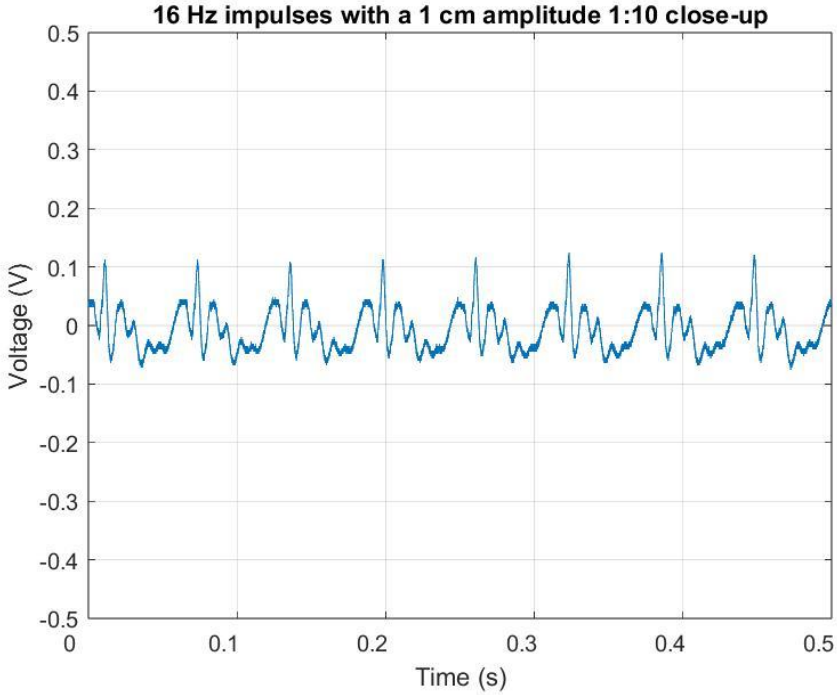

g – *A 16 Hz voltage signal wave 1:10 close-up*

h

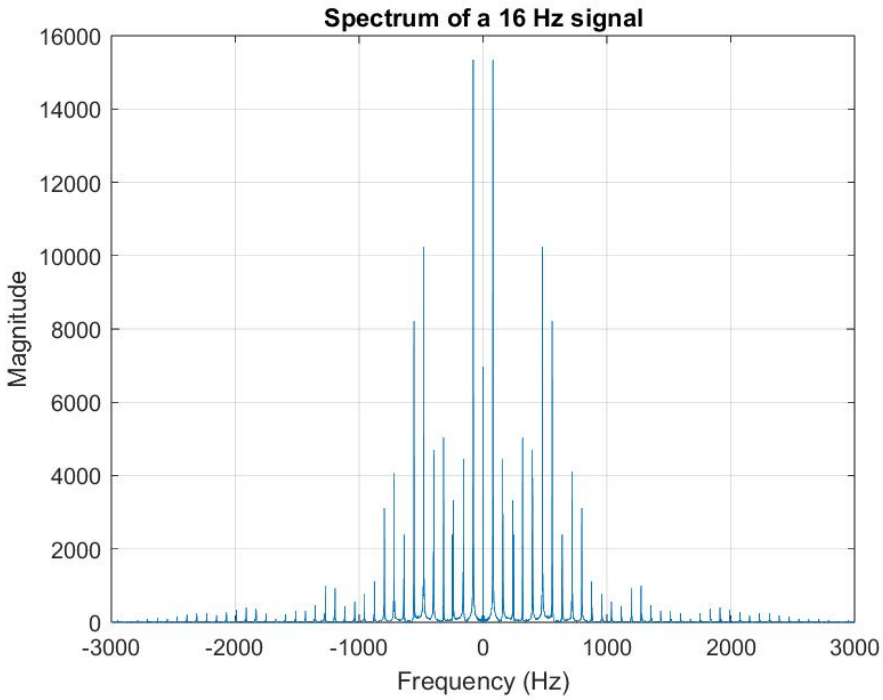

h – *A 16 Hz voltage signal spectrum*